BMC Cardiovascular Disorders

RESEARCH

Open Access

Comparison between compressed sensing and segmented cine cardiac magnetic resonance: a meta-analysis

Jason Craft[1*], Yulee Li[1], Niloofar Fouladi Nashta[2] and Jonathan Weber[1]

Abstract

Purpose Highly accelerated compressed sensing cine has allowed for quantification of ventricular function in a single breath hold. However, compared to segmented breath hold techniques, there may be underestimation or overestimation of LV volumes. Furthermore, a heterogeneous sample of techniques have been used in volunteers and patients for pre-clinical and clinical use. This can complicate individual comparisons where small, but statistically significant differences exist in left ventricular morphological and/or functional parameters. This meta-analysis aims to provide a comparison of conventional cine versus compressed sensing based reconstruction techniques in patients and volunteers.

Methods Two investigators performed systematic searches for eligible studies using PubMed/MEDLINE and Web of Science to identify studies published 1/1/2010-3/1/2021. Ultimately, 15 studies were included for comparison between compressed sensing cine and conventional imaging.

Results Compared to conventional cine, there were small, statistically significant overestimation of LV mass, underestimation of stroke volume and LV end diastolic volume (mean difference 2.65 g [CL 0.57–4.73], 2.52 mL [CL 0.73–4.31], and 2.39 mL [CL 0.07–4.70], respectively). Attenuated differences persisted across studies using prospective gating (underestimated stroke volume) and non-prospective gating (underestimation of stroke volume, overestimation of mass). There were no significant differences in LV volumes or LV mass with high or low acceleration subgroups in reference to conventional cine except slight underestimation of ejection fraction among high acceleration studies. Reduction in breath hold acquisition time ranged from 33 to 64%, while reduction in total scan duration ranged from 43 to 97%.

Conclusion LV volume and mass assessment using compressed sensing CMR is accurate compared to conventional parallel imaging cine.

Keywords Review article, Compressed sensing, Real-time cine, Cine MRI

*Correspondence:
Jason Craft
Jason.Craft@chsli.org
[1]DeMatteis Cardiovascular Institute, St. Francis Hospital & Heart Center, 100 Port Washington Blvd, Roslyn, NY 11576, USA
[2]Sol Price School of Public Policy and Leonard D. Schaeffer Center for Health Policy and Economics, University of Southern California, Los Angeles, CA, USA

Introduction

Cardiac MRI (CMR) is the gold standard for quantification of left ventricular volume and function [1]. However, balanced steady-state free precession (bSSFP) segmented cardiac cine is prone to corruption by cardiac and respiratory motion. Conventional parallel imaging techniques have led to a shorter breath hold duration at an expense of signal to noise, but do not address the limitations of the segmented technique. Real-time cine imaging with conventional parallel imaging is not sufficient in many instances, sacrificing spatial, temporal resolution, and overall image fidelity. Over the last few years, compressed sensing (CS) cardiac cine entered the investigational phase and now is commercially available. Therefore, CS cine has served to meet a clinical need, giving clinicians the ability to image critically ill patients with limited cardiorespiratory reserve. Despite the overall high quality of CS cine, some previous studies have suggested statistically significant difference trends in left and/or right ventricular volumetric data, while others have not [2–16]. Historically, several sampling algorithms and reconstruction techniques have been explored. However, only a select few have been established and been made available for on-scanner reconstruction, and thus clinical use. Therefore, the purpose of this meta-analysis is to summarize the expected differences in left ventricular structure and function parameters using clinically feasible CS cine versus the reference breath hold cine.

Methods

Search Strategy

This study followed the recommendations of the preferred reporting items for systematic reviews and meta-analyses statement (PRISMA). Two investigators (NFN and JC) performed systematic searches for eligible studies using PubMed/MEDLINE and Web of Science to identify studies published between 1/1/2010 and 3/1/2021. Search terms included "compressed sense cine," "compressed sensing cine," and "compressed sensing cine NOT Non-iterative reconstructions."

Study selection

First, titles and abstracts found by searches were assessed for eligibility by one author and verified by another (NFN and JW). After consensus was reached, full texts of preliminarily eligible studies were extracted and independently assessed by two investigators (JC and JW) against criteria for final inclusion. Study quality was independently evaluated by two authors (JC and JW) using the COSMIN Risk of Bias tool to assess the quality of studies on reliability and measurement error of outcome measurement instrument scale [17].

Inclusion criteria

Studies used for the purpose of this meta-analysis compared reference segmented bSSFP vs. CS cine. Numerous approaches to CS reconstruction have been employed to accelerate cine imaging in pre-clinical and clinical CMR.

Table 1 Study-specific differences in left ventricular ejection fraction

Study name	Sample Size	Standardized difference	95% CL	p value	Mean difference, (%)	95% CL	p value	Weight
Allen, et al. Int J Cardiovasc Imaging 2016 [2]	29	0.08	(-0.66, 0.82)	0.840	0.70	(-6.11, 7.51)	0.840	1.3
Ma et al. Clinical Radiology 2019 [3]	33	-0.32	(-0.67, 0.03)	0.073	-0.40	(-0.83, 0.03)	0.066	5.6
Kido et al. JCMR 2021 [4]	65	-0.20	(-0.45, 0.04)	0.104	-1.10	(-2.41, 0.21)	0.101	11.4
Kido et al. JCMR 2016 [5]	81	-0.03	(-0.47, 0.41)	0.903	-0.40	(-6.82, 6.02)	0.903	3.6
Goebel et al. JMRI 2016 [6]	16	-0.18	(-0.68, 0.31)	0.470	-2.00	(-7.38, 3.38)	0.466	2.8
Goebel et al. Eur Radiology 2016 [7]	26	-0.38	(-1.16, 0.39)	0.336	-4.00	(-12.07, 4.07)	0.332	1.1
Goebel et al. Acta Radiology 2017 [8]	20	-0.37	(-0.83, 0.08)	0.106	-3.80	(-8.25, 0.65)	0.094	3.3
Allen, et al. Eur Radiology 2018 [9]	27	0.07	(-0.7, 0.84)	0.863	0.90	(-9.34, 11.14)	0.863	1.2
Sudarski et al. Radiology 2016, [10] Patients	50	-0.29	(-0.57, -0.01)	0.046	-1.00	(-1.96, -0.04)	0.042	8.6
Sudarski et al. Radiology 2016, [10] Ctrl subjects	10	-0.17	(-0.8, 0.45)	0.592	-0.80	(-3.7, 2.1)	0.589	1.8
Naresh et al. Pediatric Radiology 2020 [11]	28	0.07	(-0.3, 0.44)	0.704	2.00	(-8.32, 12.32)	0.704	5.0
Kocaoglu et al. J Cardiovasc Magn Reson 2020 [12]	26	0.07	(-0.31, 0.46)	0.716	0.20	(-0.88, 1.28)	0.716	4.6
Wang et al. SS CS Cardiovasc Diagn Ther 2020 [13]	38	-0.04	(-0.36, 0.28)	0.800	-0.40	(-3.5, 2.7)	0.800	6.8
Wang et al. 2-shot SS Cardiovasc Diagn Ther 2020 [13]	38	0.02	(-0.3, 0.33)	0.923	0.10	(-1.93, 2.13)	0.923	6.8
Wang et al. Int J Cardiovasc Imaging 2020 [14]	121	0.00	(-0.18, 0.18)	1.000	0.00	(-0.06, 0.06)	1.000	21.6
Lin et al. J Magn Reson Imaging 2017 [15]	50	0.16	(-0.12, 0.44)	0.261	0.40	(-0.29, 1.09)	0.258	8.8
Vincenti et al. JACC Cardiovasc Imaging 2014 [16]	33	-0.30	(-0.65, 0.05)	0.089	-1.30	(-2.77, 0.17)	0.082	5.6
Pooled (random effects) model		-0.09	(-0.17, -0.01)	0.038	-0.20	(-0.47, 0.06)	0.134	

Differences in LVEF between compressed-sensing and control sequences are presented as standardized difference and mean difference with effects pooled using a random effects model

To ensure relevance and compatibility with everyday clinical practice, only Cartesian data sampling methods with on-scanner reconstruction were considered. These typically included a pseudo-random sampling strategy in k-t space, an iterative SENSE (sensitivity encoding)-like reconstruction algorithm, and a CS sparsity constraint along the k-space phase encoding direction and the temporal space [18–20].

Exclusion criteria

Studies using radial, spiral, or other alternative k-space trajectories and reconstruction algorithms not available for clinical use because of lengthy and/or offline reconstruction were excluded. This removes some degree of heterogeneity across studies.

Statistical analysis

Variables extracted for analysis from full texts included CS cine and reference left ventricular end-systolic (LVESV) and end-diastolic volumes (LVEDV), stroke volume (LVSV), ejection fraction (LVEF), and mass (LVM). Data formats extracted included raw group means/standard deviation, or mean differences/mean difference standard deviation. Volumetric variables and mass of CS cine sequences were compared with control sequences. Comparisons were displayed as CS measurement minus reference measurement whereas underestimation and overestimation by CS sequences is displayed as negative or positive differences, respectively. Mean differences and standardized differences were presented and pooled analyses were performed using random-effect models. I^2 tests for heterogeneity were performed for each volumetric variable and mass whereby I^2 values of $>50\%$ were considered substantial according to the Cochrane handbook. Publication bias was assessed through the use of funnel plots with the trim-and-fill method along with Egger's test and Kendall's Tau. Two-sided p values <0.05 were considered statistically significant. All analyses were performed using Comprehensive Meta Analysis software version 3 (Biostat Inc., Englewood, NJ).

Results

There were 149 studies found in initial searches. After screening titles and abstracts for eligibility, 51 full-text studies were extracted and assessed. There were 15 studies which met study inclusion criteria. 1 study included two entirely separate CS evaluations and was included twice in pooled analyses (Fig. 1). There were 5 studies with missing data required for comparison among which 2 study were included after contacting co-authors for missing information. One study presented healthy control subjects and disease subjects separately.

Study specific acquisition parameters

CS cine acquisition parameters and details for each study are displayed in tables S1 and S2 of the online supplement. All 15 studies used an online CS cine prototype developed with a CS technique combined with SENSE. These prototypes featured a pseudo-random sampling trajectory in k-t space and an iterative reconstruction algorithm. Among them, 12 were implemented on Siemens MRI scanners and 3 on Philips MRI scanners. The median sample size was 33 (range 16–121). Seven studies used CS prospective gating (segmented or single shot), six studies used ungated CS real-time acquisitions (no EKG) or retrospective (segmented) gating; one study used both retrospective/prospective gating; and one study was unknown. There were 9 studies which included papillary muscle in volumetric analyses while 1 excluded and 5 were not reported. Acceleration factors ranged from 2.5 to 13. Notably, 8 studies were performed on 1.5T MRI systems with the remaining performed on 3T systems. Compared with the control sequences, CS cine resulted in a reduction in overall scan time of between 43 and 97%, with a reduction of breath hold duration (when applicable) ranging from 33 to 64%.

Global differences in LV mass, volumes, and analysis of gating

Pooled mean differences between CS cine sequences and control sequences are reported in Fig. 2 for LV volumes, LVEF, and LVM using random-effects models. Underestimation by CS cine sequences of LVEDV (by 2.4 mL) and LVSV (by 2.5 mL), and slight overestimation of LVM (by 2.7 g) were found to be statistically significant ($p<0.05$). Study-specific comparisons including mean differences and standardized differences are reported in Tables 1, 2, 3, 4 and 5. The I^2 values were in the range of 3–30%, indicating likely non-significant heterogeneity. Risk of bias evaluated using the COSMIN checklist yielded very consistent results between raters. Risk of bias in individual studies appears low with all bias metrics ranked as "very good" or "adequate" by both raters. Risk of publication bias evaluated through the use of funnel plots and the trim-and-fill method yielded bias-corrected results very similar to original standard differences. Interdependence of variance and effect size as well as asymmetry of the funnel plots were also not found through the use of Kendall's tau and Egger's test, respectively (table S3 of the online supplement). Subgroup analyses among studies using prospective vs. non prospective gating are reported in Figs. 3 and 4. Again, there is redemonstration of statistically significant but attenuated minimal differences in LVSV for prospectively gated studies, and LVSV and LVM for non-prospective or non-gated studies.

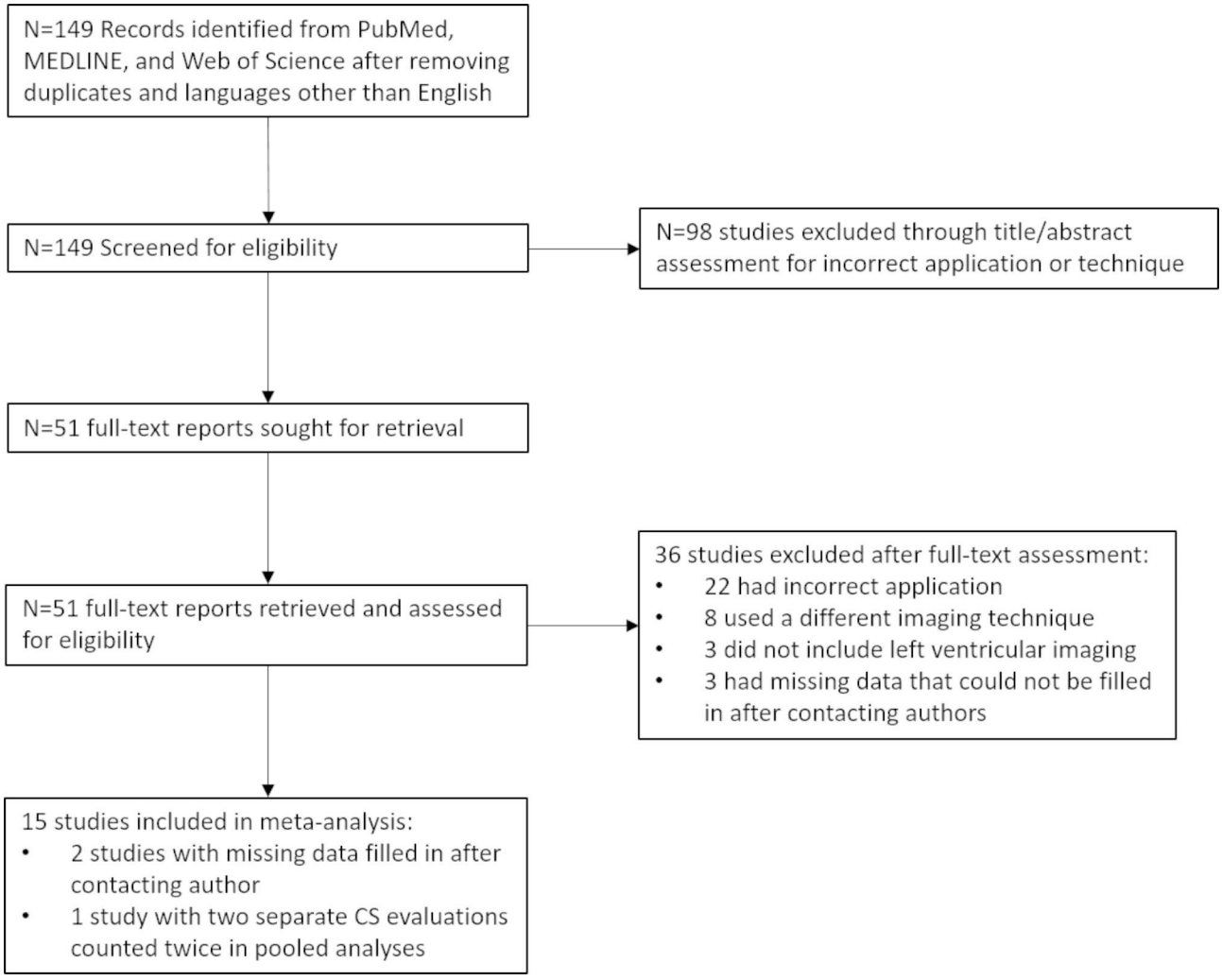

Fig. 1 PRISMA flow-chart.
There were 15 studies included in the meta-analysis after screening 149 records from PubMed, MEDLINE and Web of Science. There were 2 studies whose missing data was filled in after contacting authors and 1 study that contributed two sets of compressed sensing comparisons and was included twice in pooled analyses

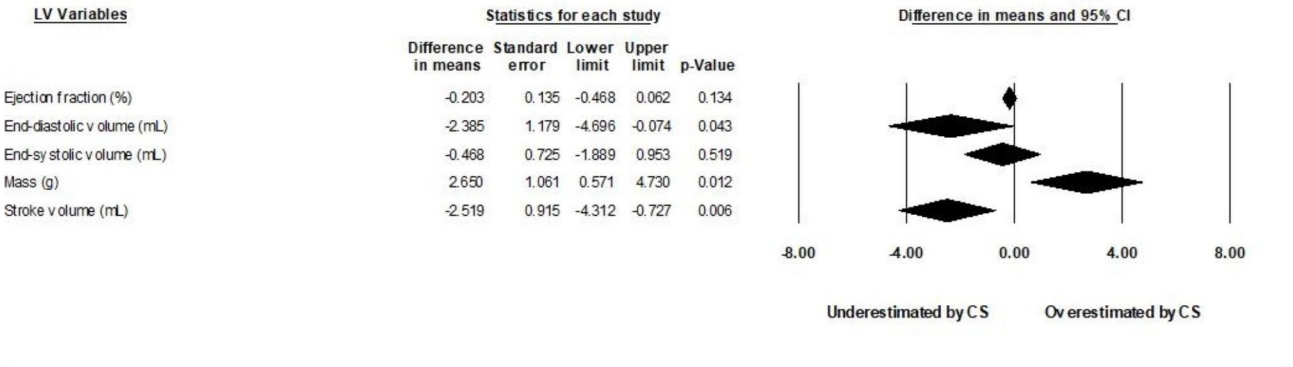

Fig. 2 Pooled results, all studies.
Comparison between compressed-sensing and control sequences. Pooled comparisons of left ventricular parameters between compressed-sensing and control sequences among included studies demonstrated small, statistically significant differences underestimations of LVEDV and LVSV, as well as slight overestimation of LV mass compared with the reference group ($p \leq 0.05$)

Table 2 Study-specific differences in left ventricular end-diastolic volume

Study name	Sample Size	Standardized difference	95% CL	p value	Mean difference, mL	95% CL	p value	Weight
Allen, et al. Int J Cardiovasc Imaging 2016 [2]	29	0.13	(-0.61, 0.88)	0.722	6.80	(-30.68, 44.28)	0.722	3.2
Ma et al. Clinical Radiology 2019 [3]	33	-0.06	(-0.4, 0.28)	0.726	-0.23	(-1.51, 1.05)	0.725	6.8
Kido et al. JCMR 2021 [4]	65	-0.04	(-0.28, 0.21)	0.771	-0.30	(-2.32, 1.72)	0.771	8.0
Kido et al. JCMR 2016 [5]	81	-0.03	(-0.47, 0.41)	0.900	-1.20	(-19.94, 17.54)	0.900	5.7
Goebel et al. JMRI 2016 [6]	16	-0.13	(-0.62, 0.36)	0.611	-5.60	(-27.12, 15.92)	0.610	5.1
Goebel et al. Eur Radiology 2016 [7]	26	-0.15	(-0.92, 0.62)	0.706	-6.00	(-37.18, 25.18)	0.706	3.0
Goebel et al. Acta Radiology 2017 [8]	20	0.32	(-0.13, 0.77)	0.166	5.90	(-2.25, 14.05)	0.156	5.5
Allen, et al. Eur Radiology 2018 [9]	27	-0.18	(-0.95, 0.59)	0.640	-9.40	(-48.7, 29.9)	0.639	3.0
Sudarski et al. Radiology 2016, [10] Patients	50	-0.22	(-0.5, 0.06)	0.130	-1.90	(-4.33, 0.53)	0.125	7.5
Sudarski et al. Radiology 2016, [10] Ctrl subjects	10	-0.07	(-0.69, 0.55)	0.823	-0.60	(-5.85, 4.65)	0.823	4.0
Naresh et al. Pediatric Radiology 2020 [11]	28	-0.07	(-0.44, 0.3)	0.706	-2.00	(-12.36, 8.36)	0.705	6.4
Kocaoglu et al. J Cardiovasc Magn Reson 2020 [12]	26	-0.29	(-0.68, 0.1)	0.148	-2.00	(-4.65, 0.65)	0.139	6.2
Wang et al. SS CS Cardiovasc Diagn Ther 2020 [13]	38	0.07	(-0.25, 0.38)	0.686	1.00	(-3.84, 5.84)	0.685	7.1
Wang et al. 2-shot SS Cardiovasc Diagn Ther 2020 [13]	38	0.06	(-0.26, 0.38)	0.706	0.70	(-2.93, 4.33)	0.705	7.1
Wang et al. Int J Cardiovasc Imaging 2020 [14]	121	0.02	(-0.16, 0.2)	0.847	1.30	(-11.92, 14.52)	0.847	8.7
Lin et al. J Magn Reson Imaging 2017 [15]	50	-0.91	(-1.24, -0.58)	0.000	-14.80	(-19.32, -10.28)	0.000	6.9
Vincenti et al. JACC Cardiovasc Imaging 2014 [16]	33	-0.97	(-1.38, -0.56)	0.000	-9.90	(-13.38, -6.42)	0.000	5.9
Pooled (random effects) model		-0.15	(-0.32, 0.01)	0.059	-2.39	(-4.7, -0.07)	0.043	

Differences in LVEDV between compressed-sensing and control sequences are presented as standardized difference and mean difference with effects pooled using a random effects model

Table 3 Study-specific differences in left ventricular end-systolic volume

Study name	Sample Size	Standardized difference	95% CL	p value	Mean difference, mL	95% CL	p value	Weight
Allen, et al. Int J Cardiovasc Imaging 2016 [2]	29	0.09	(-0.65, 0.83)	0.816	2.70	(-20.08, 25.48)	0.816	2.6
Ma et al. Clinical Radiology 2019 [3]	33	0.24	(-0.11, 0.58)	0.178	0.39	(-0.17, 0.95)	0.172	6.8
Kido et al. JCMR 2021 [4]	65	0.05	(-0.2, 0.29)	0.706	0.30	(-1.26, 1.86)	0.705	8.7
Kido et al. JCMR 2016 [5]	81	-0.01	(-0.44, 0.43)	0.982	-0.20	(-17.71, 17.31)	0.982	5.3
Goebel et al. JMRI 2016 [6]	16	0.08	(-0.41, 0.57)	0.743	1.30	(-6.47, 9.07)	0.743	4.7
Goebel et al. Eur Radiology 2016 [7]	26	0.11	(-0.66, 0.88)	0.776	3.00	(-17.6, 23.6)	0.775	2.4
Goebel et al. Acta Radiology 2017 [8]	20	0.62	(0.14, 1.1)	0.011	8.60	(2.56, 14.64)	0.005	4.8
Allen, et al. Eur Radiology 2018 [9]	27	-0.41	(-1.19, 0.37)	0.299	-25.40	(-72.82, 22.02)	0.294	2.4
Sudarski et al. Radiology 2016, [10] Patients	50	-0.08	(-0.36, 0.2)	0.577	-0.80	(-3.61, 2.01)	0.577	8.0
Sudarski et al. Radiology 2016, [10] Ctrl subjects	10	0.28	(-0.35, 0.92)	0.377	2.90	(-3.41, 9.21)	0.368	3.3
Naresh et al. Pediatric Radiology 2020 [11]	28	-0.09	(-0.46, 0.28)	0.642	-3.00	(-15.61, 9.61)	0.641	6.3
Kocaoglu et al. J Cardiovasc Magn Reson 2020 [12]	26	-0.27	(-0.66, 0.12)	0.172	-1.20	(-2.89, 0.49)	0.164	6.0
Wang et al. SS CS Cardiovasc Diagn Ther 2020 [13]	38	0.07	(-0.24, 0.39)	0.649	0.90	(-2.97, 4.77)	0.648	7.2
Wang et al. 2-shot SS Cardiovasc Diagn Ther 2020 [13]	38	0.01	(-0.31, 0.33)	0.955	0.10	(-3.38, 3.58)	0.955	7.3
Wang et al. Int J Cardiovasc Imaging 2020 [14]	121	0.02	(-0.16, 0.2)	0.832	0.80	(-6.57, 8.17)	0.832	10.0
Lin et al. J Magn Reson Imaging 2017 [15]	50	-0.74	(-1.06, -0.43)	0.000	-8.40	(-11.53, -5.27)	0.000	7.3
Vincenti et al. JACC Cardiovasc Imaging 2014 [16]	33	-0.17	(-0.51, 0.17)	0.330	-2.00	(-5.99, 1.99)	0.326	6.8
Pooled (random effects) model		-0.03	(-0.16, 0.11)	0.679	-0.47	(-1.89, 0.95)	0.519	

Differences in LVESV between compressed-sensing and control sequences are presented as standardized difference and mean difference with effects pooled using a random effects model

Analysis of acceleration factor

Finally, to study the effect of acceleration rate on quantitative parameters, the 12 Siemens CS studies were divided into 4 studies with exclusively low (<11) acceleration factors, and six studies with exclusively high (≥11) acceleration factors. One study used both high and low acceleration factors; the remaining study did not state an overall acceleration factor (could not be determined). The results are provided in Figs. 5 and 6. There were no statistically significant differences in LVM, LVEDV, LVSV,

Table 4 Study-specific differences in left ventricular mass

Study name	Sample Size	Standardized difference	95% CL	p value	Mean difference, g	95% CL	p value	Weight
Allen, et al. Int J Cardiovasc Imaging 2016 [2]	29	0.14	(-0.6, 0.88)	0.712	5.20	(-22.39, 32.79)	0.712	3.9
Ma et al. Clinical Radiology 2019 [3]	33	-0.12	(-0.46, 0.22)	0.495	-0.51	(-1.97, 0.95)	0.494	8.0
Kido et al. JCMR 2021 [4]	65	-0.15	(-0.4, 0.09)	0.221	-0.90	(-2.33, 0.53)	0.219	9.3
Kido et al. JCMR 2016 [5]	81	-0.04	(-0.48, 0.39)	0.845	-1.20	(-13.23, 10.83)	0.845	6.8
Goebel et al. JMRI 2016 [6]	16	0.27	(-0.23, 0.77)	0.287	9.30	(-7.53, 26.13)	0.279	6.0
Goebel et al. Eur Radiology 2016 [7]	26	0.06	(-0.71, 0.83)	0.877	2.00	(-23.33, 27.33)	0.877	3.7
Goebel et al. Acta Radiology 2017 [8]	20	0.22	(-0.22, 0.67)	0.323	2.70	(-2.59, 7.99)	0.317	6.7
Allen, et al. Eur Radiology 2018 [9]	27	0.21	(-0.56, 0.99)	0.585	6.00	(-15.47, 27.47)	0.584	3.7
Sudarski et al. Radiology 2016, [10] Patients	50	0.89	(0.56, 1.22)	0.000	8.70	(5.99, 11.41)	0.000	8.2
Sudarski et al. Radiology 2016, [10] Ctrl subjects	10	1.39	(0.52, 2.26)	0.002	10.40	(5.75, 15.05)	0.000	3.1
Kocaoglu et al. J Cardiovasc Magn Reson 2020 [12]	26	0.47	(0.06, 0.87)	0.024	2.00	(0.35, 3.65)	0.018	7.2
Wang et al. SS CS Cardiovasc Diagn Ther 2020 [13]	38	0.04	(-0.28, 0.36)	0.818	0.90	(-6.74, 8.54)	0.817	8.3
Wang et al. 2-shot SS Cardiovasc Diagn Ther 2020 [13]	38	0.05	(-0.27, 0.36)	0.778	0.80	(-4.76, 6.36)	0.778	8.3
Lin et al. J Magn Reson Imaging 2017 [15]	50	0.08	(-0.2, 0.35)	0.590	0.90	(-2.37, 4.17)	0.590	8.9
Vincenti et al. JACC Cardiovasc Imaging 2014 [16]	33	0.26	(-0.09, 0.61)	0.141	2.50	(-0.78, 5.78)	0.135	7.9
Pooled (random effects) model		0.20	(0.02, 0.38)	0.026	2.65	(0.57, 4.73)	0.012	

Differences in LVM between compressed-sensing and control sequences are presented as standardized difference and mean difference with effects pooled using a random effects model

Table 5 Study-specific differences in left ventricular stroke volume

Study name	Sample Size	Standardized difference	95% CL	p value	Mean difference, mL	95% CL	p value	Weight
Allen, et al. Int J Cardiovasc Imaging 2016 [2]	29	0.16	(-0.59, 0.9)	0.681	4.80	(-18.05, 27.65)	0.681	3.9
Ma et al. Clinical Radiology 2019 [3]	33	-0.20	(-0.55, 0.14)	0.246	-0.62	(-1.66, 0.42)	0.241	10.5
Kido et al. JCMR 2021 [4]	65	-0.06	(-0.3, 0.18)	0.622	-0.60	(-2.98, 1.78)	0.622	13.8
Kido et al. JCMR 2016 [5]	81	-0.06	(-0.5, 0.38)	0.796	-1.00	(-8.58, 6.58)	0.796	8.2
Goebel et al. Eur Radiology 2016 [7]	26	-0.45	(-1.23, 0.33)	0.257	-10.00	(-27.09, 7.09)	0.251	3.6
Goebel et al. Acta Radiology 2017 [8]	20	-0.16	(-0.6, 0.28)	0.486	-2.90	(-11, 5.2)	0.483	8.1
Allen, et al. Eur Radiology 2018 [9]	27	-0.10	(-0.87, 0.67)	0.791	-2.20	(-18.5, 14.1)	0.791	3.7
Sudarski et al. Radiology 2016, [10] Patients	50	-0.26	(-0.54, 0.02)	0.074	-2.30	(-4.78, 0.18)	0.069	12.5
Sudarski et al. Radiology 2016, [10] Ctrl subjects	10	0.01	(-0.61, 0.63)	0.967	0.10	(-4.66, 4.86)	0.967	5.2
Kocaoglu et al. J Cardiovasc Magn Reson 2020 [12]	26	-0.16	(-0.54, 0.23)	0.432	-0.90	(-3.13, 1.33)	0.429	9.4
Lin et al. J Magn Reson Imaging 2017 [15]	50	-0.75	(-1.07, -0.44)	0.000	-6.40	(-8.76, -4.04)	0.000	11.5
Vincenti et al. JACC Cardiovasc Imaging 2014 [16]	33	-0.68	(-1.06, -0.3)	0.000	-8.70	(-13.07, -4.33)	0.000	9.6
Pooled (random effects) model		-0.26	(-0.42, -0.1)	0.002	-2.52	(-4.31, -0.73)	0.006	

Differences in LVSV between compressed-sensing and control sequences are presented as standardized difference and mean difference with effects pooled using a random effects model

LVESV, or observed compared to the gold standard. LVEF measured in high acceleration factor studies was slightly underestimated (1.08%, p = 0.001) by CS cine sequences.

Discussion

Development of compressed sensing and parallel imaging

Parallel imaging was developed in the late 1990s after the availability of radiofrequency coil arrays [21]. This method can accelerate segmented cine CMR by undersampling k-space. A special image reconstruction algorithm is used which can either suppress image-space aliasing artifacts caused by k-space undersampling or recover missing k-space data directly. Two representative parallel imaging techniques are SENSE [22] and GRAPPA [23]. SENSE is an image-space reconstruction technique that can suppress aliasing artifacts by directly using multi-channel coil sensitivity encoding. GRAPPA is a k-space technique that can implicitly utilize multi-channel coil sensitivity encoding to calibrate k-space data relationship for data recovery. Both SENSE and GRAPPA use cartesian sampling with a linear reconstruction algorithm, providing a practically effective and computationally affordable method for segmented cine. Because segmented cine data are collected dynamically, they can

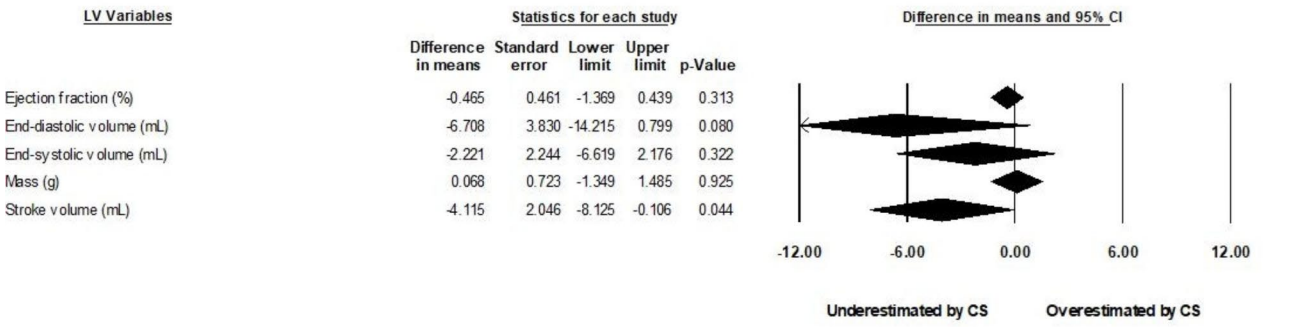

Fig. 3 Subgroup analysis results, prospective gating.
Comparison of sequences stratified by gating method. Left ventricular parameter comparisons stratified by prospective gating yielded similar but attenuated underestimation of stroke volume

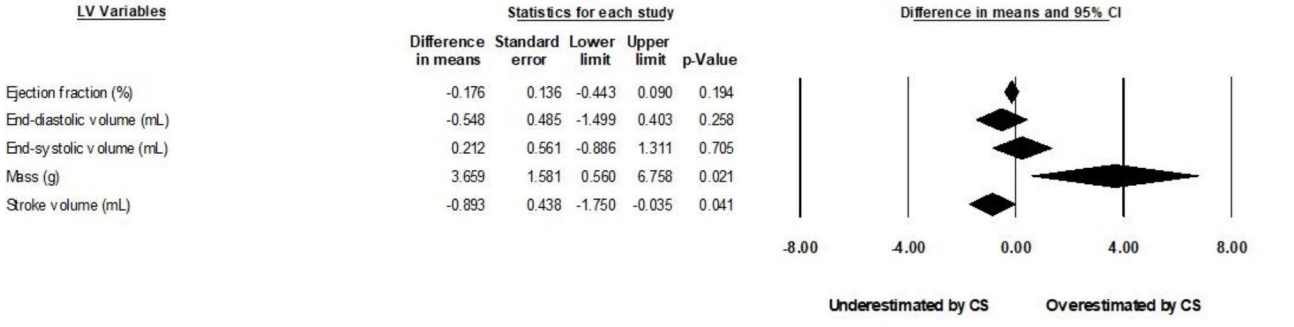

Fig. 4 Subgroup analysis results, non-prospective gating or no gating.
Comparison of sequences stratified by gating method. Ungated/retrospective gating demonstrated slight overestimation of LV mass and underestimation of LVSV compared with reference

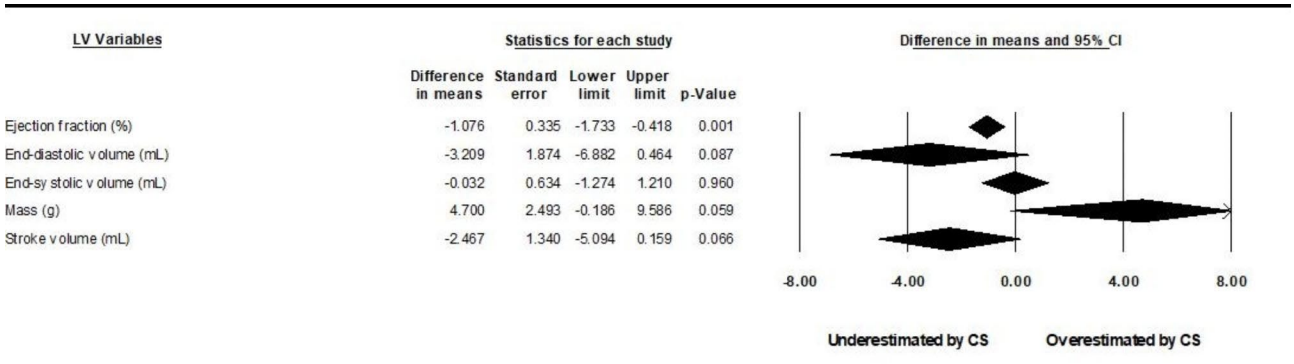

Fig. 5 Subgroup analysis results, high acceleration factor (≥ 11).
Comparison of sequences stratified by acceleration factor. High (≥ 11) acceleration factor CS sequences demonstrated non-significant differences except slightly underestimated LVEF

benefit from time-domain data correlation. This enables a set of k-t space acceleration techniques, including k-t GRAPPA [24] and k-t SENSE/BLAST [25], for further imaging acceleration.

CS reconstruction was introduced for MRI applications more recently in the 2000s [26]. This method relies on data sparsity naturally existing in medical images. A random sampling strategy is required for generating

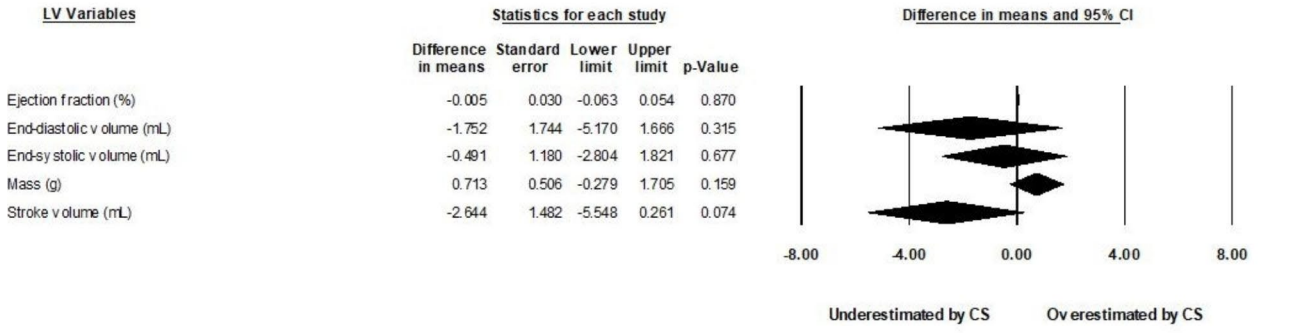

Fig. 6 Subgroup analysis results, low acceleration factor (< 11).
Low (< 11) acceleration factor sequences demonstrated attenuated non-significant differences compared with all pooled studies

incoherence of undersampling artifacts in image space. By non-linearly enforcing both image sparsity and data consistency with the acquired samples, the image artifacts can be effectively suppressed. Because cardiac images have high sparsity in k-t space, CS found applications rapidly in the field of CMR. CS cine was developed to overcome two challenges in conventional segmented cine: first, breath holding is difficult in many heart patients; second, ECG synchronization for data segmentation may not be effective for arrhythmia patients. Ideally, CS cine would accelerate CMR beyond parallel imaging that is limited by MRI coil array, thereby allowing for real-time cine with free breathing. However, CS cine may lower image resolution because sparsity enforcement may smooth the images either in image space or along the time. Because CS requires random sampling, it is suitable for non-Cartesian sampling trajectories that naturally produce noise-like (incoherent) aliasing artifacts. However, non-Cartesian sampling may suffer from k-space trajectory inaccuracy due to gradient imperfection, manifesting as image blurs or distortion. For this reason, Cartesian sampling is preferred in clinical applications. Cartesian CS typically uses pseudo-random sampling in k-space [27–29]. The reconstruction algorithm is non-linear and iterative, thereby requiring more reconstruction time than parallel imaging. A high-performance computer is usually needed for CS reconstruction in a clinical environment.

Iterative SENSE and CS SENSE

Many research studies have combined parallel imaging and CS together [30, 31], making it possible to take advantage of both multi-channel coil sensitivity encoding and image sparsity in imaging acceleration. To that end, iterative SENSE has been found to be useful because it features an iterative algorithm and an arbitrary sampling trajectory [32] that are both needed for the application of CS sparsity constraint. In the presented work, all the 15 studies relied on the CS combined with iterative SENSE. The Cartesian data were sampled with higher density around the central k-space than that in the peripheral k-space. This variable density sampling allowed for image reconstruction without reference scans like in SENSE and thus improved overall imaging acceleration. It was reported that the combination of CS and SENSE provided high acceleration factor (typically ≥ 8) without considerable loss in image resolution. However, these CMR cine prototypes required significant computation in image reconstruction. To reduce reconstruction time, the algorithm is now implemented practically with graphic processing unit (GPU) [33]. This has fulfilled clinical needs in most cases with a higher cost on computer hardware.

Overview: reproducibility of measurements

To our knowledge, this is the first meta-analysis comparing CS cine with the gold standard bSSFP segmented cine. Several factors can influence the reproducibility of left and right ventricular volumetric measurements. Miller et al. showed the ideal spatial resolution for cardiac cine was < 2 mm, with a temporal resolution ≤ 45 ms [34]. With decreasing temporal resolution (reduction in the number of true cine frames) on segmented sequences, true end systole could be missed, leading to an overestimation of LVESV and underestimation of LVEF. Decreasing spatial resolution was associated with increased LVEDV. True voxel size up to 3 mm and true cine frame intervals up to 90 ms were not shown to affect LVM. All included studies met the former specification for acceptable spatial and temporal resolution; however, several studies have noted significant differences in left ventricular volumetric data as well as LVM compared to the reference. These differences included underestimation as well as overestimation of LVEDV, LVESV, LVSV and LVM. The net effect of the meta-analysis has shown overall, although statistically significant differences in

LVSV, LVEDV, and LVM exist, they are unlikely to be clinically impactful.

Effect of gating method

Because of the inherent trigger delay with prospective gating, true end-diastole is not captured, resulting in smaller end diastolic volumes, stroke volumes, and ejection fractions [35]. Alternatively, retrospective and real-time imaging also became feasible without the use of offline reconstruction. Ungated sequences could be of particular value at higher field strengths given the burden of magnetohydrodynamic effects on EKG T-wave amplitude.

Differences in LVM persisted across several studies with different gating methods. Individual author observations included the following: Sudarski et al. identified overestimation of LVM with prospective gating. Kocaoglu et al. noted overestimation of LVM using breath hold CS cine vs. reference, but no significant difference in free breathing CS cine vs. reference. After indexing for BSA, there was no significant difference between breath hold CS cine and reference. Kido et al. [JCMR, 2016] noted underestimation of LVM with CS cine using prospective gating covering>1 cardiac cycle. Ma et al. noted underestimation in LVM with CS cine using retrospective gating. In several studies, CS cine showed increased or decreased LVEDV, LVSV, LVEF, and increased LVESV regardless of gating method used. In our subgroup analyses however, prospectively gated CS cine sequence studies demonstrated no significant differences between LV volumes and mass except for LVSV which was slightly underestimated.

Image contrast, spatial-temporal blurring, and post-processing

Acceleration factors

CS substantially improves quality of real-time imaging, which may be comparable to the reference based on several of the included studies. Increased spatial-temporal undersampling occurs at higher acceleration factors. As mentioned, tradeoffs for consideration include decreased image contrast, temporal blurring, and decreased image sharpness which is linked to the degree of undersampling. Alternatively, CS cine with segmented imaging can be used with a substantially shortened breath hold duration using a smaller acceleration factor. The studies in this meta-analysis used an acceleration factor ranging from 2.5 to 4 for the CS cine prototypes on the Philips MRI scanners, and 4-12.8 for the CS cine prototypes on the Siemens MRI scanners. In the group of Siemens CS cine prototypes, differences in LV volumes/and or mass occurred in studies with acceleration rates of >=11 (high) regardless of gating method (total 6 of 12 studies). 4 out of 12 studies exclusively used acceleration rates<11 (low) and showed no difference compared to reference[2, 13, 14]. Only one study from the high acceleration pool showed no significant difference vs. reference[5]. One study contained high and low acceleration rates and showed no difference[9]; one study only included differential subsampling rates so the overall acceleration factor could not be determined[6]. In the group of Philips CS cine prototypes, only 3 studies were included that used the CS-SENSE method[3, 11, 12]. Statistically significant differences in left ventricular quantitative parameters were present in 2 studies using the acceleration rates of 3 and 4 compared to 2.5-3.5x acceleration. Due to the relatively small number of studies on the Philips MRI scanners, subgroup analysis based on acceleration rate from this vendor could not be performed. Overall, stratified subgroup-analysis based on acceleration factor could not explain the differences in the non-stratified comparison, and only a trivial underestimation in LVEF among the high acceleration group was appreciated. Low overall mean differences in stroke volume, LVEDV, and LVM in the aggregate analysis likely influenced the result of this particular subgroup analysis.

Left ventricular papillary muscles and trabeculations

Another factor affecting left ventricular quantitative measurements in clinical practice is inclusion/exclusion of the papillary muscle into the left ventricular volume or mass. Only one study definitively excluded papillary muscles from the left ventricular volume. Han et al. demonstrated papillary muscle and trabeculation inclusion resulted in a 17% higher indexed LVM, 20% lower indexed LVEDV, and 13% higher LVEF in patients with hypertrophic cardiomyopathy. Imaging at a higher spatial resolution may be necessary to successfully depict small left ventricular trabeculation and myocardial crypts if inclusion into the left ventricular mass is desired [36]. Additionally, thresholding techniques may be affected by decreased image contrast [37], and performing left ventricular cine after infusion of gadolinium based contrast agents (GBCA). These considerations may be important when using higher acceleration factors.

Potential implications of readout: GRE vs. bSSFP

The T2/T1 weighting of bSSFP and high flip angles result in a darker appearance of the myocardium compared to gradient recall echo (GRE). The flow sensitivity of GRE also affects image contrast and visualization at the sub-endocardial/blood pool interface. These factors lead to differences in volumetric measurements compared to bSSFP [38]. Due to the increased utilization of MRI in patients with MR conditional and non-conditional devices and use of higher field strengths, CS cine with GRE readout would meet a growing unmet clinical need in this population. However, decreases in

myocardial-blood pool CNR with higher acceleration factors may be more adversely impactful when combined with GRE readout.

The effect of physiologic variation

Inter-study physiologic variation must also be considered, which is particularly relevant when comparing breath hold techniques with free breathing techniques. Although image quality has been demonstrated to be adequate under these circumstances, the free breathing acquisition may introduce respiratory dependent differences in left and right ventricular volumes, introduce through plane cardiac motion, and non-matched slice positions compared to end-expiratory breath holds. On the other hand, free breathing CS offers better spatial and temporal resolution compared to conventional parallel imaging; thus, the impact of pathophysiology on ventricular filling dynamics, (i.e. interventricular dependence) can be studied with free breathing (with potentially greater sensitivity).

Barriers to CS cine adoption

As productivity and economic based concerns and incentives continue to grow and the computational processing power floor is raised, net benefit measures may favor more widespread adoption of CS cine. Some barriers to this adoption still exist, but are being addressed.

More limited data regarding the suitability of CS cine exist in the pediatric population, where there is more demand on temporal resolution, and acquired voxel size. Pediatric patients were aggregated and overall represent a small sample of patients in the included studies (2 included studies)[11, 12]. More recent studies subsequent to the search scope of this meta-analysis appear to favorably support the use of CS in this population [39]; however, some differences in LVEF and right ventricular EF compared to the reference have been appreciated [40]. Using our methodology for inclusion/exclusion, the majority of studies did not include right ventricular quantitative data (only 2 studies were representative); therefore, differences in right ventricular quantitative measurements obtained from CS cine could not be compared with the gold standard. Only one study included left ventricular strain as a variable, which was global circumferential strain[4]. Further comparisons are needed with the addition of other strain parameters such region, global longitudinal and global radial strain.

Summary of recommendations

The findings of the meta-analysis suggests that CS cine can be used for assessment of left ventricular function and volumes in certain populations. The included studies in this meta-analysis consisted mostly of adult patients. It is reasonable to conclude that longitudinal assessment with serial CMR is feasible between conventional parallel imaging and CS. Tradeoffs for consideration include patient acuity, R-R interval irregularity, need to resolve fine details that are spatial-temporal dependent (i.e. cardiac valves), post-processing technique, preservation of image contrast, workflow throughput, and evaluation of the right ventricle.

Limitations

In addition to what has already been discussed, there are some additional limitations to the present study, namely study heterogeneity. Acquisition parameters and technique varied across the studies included in the meta-analysis. This not only included spatial and temporal resolution, which have an impact on quantitative measurements, but also free breathing, breath hold, multi-shot, and single shot acquisition strategies. Given the limited number of included studies, further subgroup analysis addressing these differences could not be performed. Within the subgroup analysis performed (gating method and acceleration factor), confidence intervals were generally wider, which was due to dividing the number of studies included in the aggregate analysis. This is particularly true of the acceleration factor subgroup analysis, with a lower number of included studies compared to the gating subgroup analysis. We also acknowledge our limited ability to detect possible publication bias due to the small number of studies. Lastly, CS methods have been applied to 3D cine which can provide comparable left ventricular functional and morphological assessment [41]. The current meta-analysis only examined CS application to 2D cine.

Conclusions

CS cine provides accurate assessment of left ventricular structure and function when compared to conventional cine imaging. Small differences are observed overall in LVEDV, LVSV, and LVM.

List of Abbreviations

BLAST	Broad-use linear acquisition speed-up technique
BSA	Body surface area
bSSFP	Balance steady-state free precession
CMR	Cardiac MRI
CNR	Contrast to noise
CS	Compressed sensing
C-SENSE	Compressed SENSE
EKG	Electrocardiogram
GBCA	Gadolinium based contrast agent
GRAPPA	Generalized autocalibrating partial parallel acquisition
GRE	Gradient recall echo
LVEDV	Left ventricular end diastolic volume
LVEF	Left ventricular ejection fraction
LVESV	Left ventricular end systolic volume
LVM	Left ventricular mass
LVSV	Left ventricular stroke volume
PRISMA	Preferred reporting items for systematic reviews and meta-analyses
SENSE	Sensitivity encoding

Supplementary Information

The online version contains supplementary material available at https://doi.org/10.1186/s12872-023-03426-1.

Supplementary Material 1

Acknowledgements
The authors sincerely thank Dr. Omar Khalique and Dr. Eddy Barasch for their input regarding structure of the manuscript.

Authors' Contributions
JC is the manuscript lead was a major contributor. YL authored the manuscript and was a major contributor. NFN performed study reviews, data extraction, and was a major contributor to the study. JW was a major contributor to the manuscript and performed statistical analysis.

Funding
This work was funded by an endowment from the St. Francis Hospital Foundation.

Data Availability
Datasets analyzed for the current study were obtained from the source publications (references 2–16). However, these can be provided upon reasonable request from the corresponding author.

Declarations

Ethics approval
This study did not require ethics approval since it relies on previously published data.

Consent to participate
This study did not require informed consent since it relies on previously published data.

Consent to publish
This study did not require consent to publish since it relies on previously published data and does not present data from any one individual.

Competing interests
The authors declare no competing interests.

Received: 6 April 2023 / Accepted: 1 August 2023
Published online: 21 September 2023

References

1. Pennell DJ. Cardiovascular magnetic resonance: twenty-first century solutions in cardiology. Clin Med (Lond). 2003 May-Jun;3(3):273–8. https://doi.org/10.7861/clinmedicine.3-3-273. PMID: 12848266; PMCID: PMC4952456.
2. Allen BD, Carr M, Botelho MP, et al. Highly accelerated cardiac MRI using iterative SENSE reconstruction: initial clinical experience. Int J Cardiovasc Imaging. 2016;32(6):955–63. https://doi.org/10.1007/s10554-016-0859-3. Epub 2016 Feb 19. PMID: 26894256.
3. Ma Y, Hou Y, Ma Q, Wang X, Sui S, Wang B. Compressed SENSE single-breath-hold and free-breathing cine imaging for accelerated clinical evaluation of the left ventricle. Clin Radiol. 2019;74(4):325.e9-325.e17. doi: 10.1016/j.crad.2018.12.012. Epub 2019 Jan 25. PMID: 30686503.
4. Kido T, Hirai K, Ogawa R, et al. Comparison between conventional and compressed sensing cine cardiovascular magnetic resonance for feature tracking global circumferential strain assessment. J Cardiovasc Magn Reson. 2021;23:10. https://doi.org/10.1186/s12968-021-00708-5.
5. Kido T, Kido T, Nakamura M, et al. Compressed sensing real-time cine cardiovascular magnetic resonance: accurate assessment of left ventricular function in a single-breath-hold. J Cardiovasc Magn Reson. 2016;18(1):50. https://doi.org/10.1186/s12968-016-0271-0. PMID: 27553656; PMCID: PMC4995641.
6. Goebel J, Nensa F, Schemuth HP, et al. Compressed sensing cine imaging with high spatial or high temporal resolution for analysis of left ventricular function. J Magn Reson Imaging. 2016;44(2):366–74. https://doi.org/10.1002/jmri.25162. Epub 2016 Jan 20. PMID: 26789014.
7. Goebel J, Nensa F, Bomas B, et al. Real-time SPARSE-SENSE cardiac cine MR imaging: optimization of image reconstruction and sequence validation. Eur Radiol. 2016;26(12):4482–9. https://doi.org/10.1007/s00330-016-4301-y. Epub 2016 Mar 9. PMID: 26960537.
8. Goebel J, Nensa F, Schemuth HP, et al. Real-time SPARSE-SENSE cine MR imaging in atrial fibrillation: a feasibility study. Acta Radiol. 2017;58(8):922–8. https://doi.org/10.1177/0284185116681037. Epub 2016 Jan 1. PMID: 28273733.
9. Allen BD, Carr ML, Markl M, et al. Accelerated real-time cardiac MRI using iterative sparse SENSE reconstruction: comparing performance in patients with sinus rhythm and atrial fibrillation. Eur Radiol. 2018;28(7):3088–96. https://doi.org/10.1007/s00330-017-5283-0. Epub 2018 Jan 30. PMID: 29383529.
10. Sudarski S, Henzler T, Haubenreisser H, et al. Free-breathing sparse sampling cine MR Imaging with Iterative Reconstruction for the Assessment of Left ventricular function and Mass at 3.0 T. Radiology. 2017;282(1):74–83. https://doi.org/10.1148/radiol.2016151002. Epub 2016 Jul 11. PMID: 27399326.
11. Naresh NK, Malone L, Fujiwara T, et al. Use of compressed sensing to reduce scan time and breath-holding for cardiac cine balanced steady-state free precession magnetic resonance imaging in children and young adults. Pediatr Radiol. 2021;51(7):1192–201. https://doi.org/10.1007/s00247-020-04952-2. Epub 2021 Feb 10. PMID: 33566124.
12. Kocaoglu M, Pednekar AS, Wang H, Alsaied T, Taylor MD, Rattan MS. Breath-hold and free-breathing quantitative assessment of biventricular volume and function using compressed SENSE: a clinical validation in children and young adults. J Cardiovasc Magn Reson. 2020;22(1):54. https://doi.org/10.1186/s12968-020-00642-y. PMID: 32713347; PMCID: PMC7384228.
13. Wang J, Li X, Lin L, et al. Diagnostic efficacy of 2-shot compressed sensing cine sequence cardiovascular magnetic resonance imaging for left ventricular function. Cardiovasc Diagn Ther. 2020;10(3):431–41. https://doi.org/10.21037/cdt-20-135. PMID: 32695623; PMCID: PMC7369273.
14. Wang J, Lin Q, Pan Y, An J, Ge Y. The accuracy of compressed sensing cardiovascular magnetic resonance imaging in heart failure classifications. Int J Cardiovasc Imaging. 2020;36(6):1157–66. https://doi.org/10.1007/s10554-020-01810-y. Epub 2020 Mar 7. PMID: 32146608.
15. Lin ACW, Strugnell W, Riley R, et al. Higher resolution cine imaging with compressed sensing for accelerated clinical left ventricular evaluation. J Magn Reson Imaging. 2017;45(6):1693–9. https://doi.org/10.1002/jmri.25525. Epub 2016 Oct 26. PMID: 27783472.
16. Vincenti G, Monney P, Chaptinel J, et al. Compressed sensing single-breath-hold CMR for fast quantification of LV function, volumes, and mass. JACC Cardiovasc Imaging. 2014;7(9):882–92. https://doi.org/10.1016/j.jcmg.2014.04.016. Epub 2014 Aug 13. PMID: 25129517.
17. Lidwine B, Mokkink M, Boers et al. COSMIN Risk of Bias tool to assess the quality of studies on reliability or measurement error of outcome measurement instruments: a Delphi study. BMC Med Res Methodol. 2020;20(293).
18. Liu J, Lefebvre A, Zenge MO, et al. 2D bSSFP real-time cardiac CINE-MRI: compressed sensing featuring weighted redundant Haar Wavelet regularization in space and time. J Cardiovasc Magn Reson. 2013;15(Suppl 1):P49. http://www.jcmr-online.com/content/15/S1/P49.
19. Sartoretti T, Reischauer C, Sartoretti E, Binkert C, Najafi A, Sartoretti-Schefer S. Common artefacts encountered on images acquired with combined compressed sensing and SENSE. Insights Imaging. 2018;9(6):1107–15. https://doi.org/10.1007/s13244-018-0668-4. Epub 2018 Nov 8. PMID: 30411279; PMCID: PMC6269339.
20. Geerts-Ossevoort L, de Weerdt E, Duijndam A, van Ijperen G, Peeters H, Doneva M, Nijenhuis M, Huang A, Compressed SENSE. Speed done right. Every time. Philips Field Strength Magazine. 2018. p. 6619. https://philipsproductcontent.blob.core.windows.net/assets/20180109/619119731f2a42c4acd4a863008a46c7.pdf.
21. Roemer PB, Edelstein WA, Hayes CE, Souza SP, Mueller OM. The NMR phased array, Magn Reson Med 1990, 16(2), p192–225.
22. Pruessmann KP, Weiger M, Scheidegger MB, Boesiger P. SENSE: sensitivity encoding for fast MRI. Magn Reson Medicine: Official J Int Soc Magn Reson Med. 1999;42:952–62.
23. Griswold MA, Jakob PM, Heidemann RM, et al. Generalized autocalibrating partially parallel acquisitions (GRAPPA). Magn Reson Med. 2002;47:1202–10.

24. Tsao J, Boesiger P. Pruessmann. k-t BLAST and k-t SENSE: dynamic MRI with high frame rate exploiting spatiotemporal correlations. Magn Reson Med. 2003;50:1031–42.
25. Huang F, Akao J, Vijayakumar S, Duensing GR. Limkeman. k-t GRAPPA: a k-space implementation for dynamic MRI with high reduction factor. Magn Reson Med. 2005;54:1172–84.
26. Lustig M, Donoho D, Pauly JM, Sparse MRI. The application of compressed sensing for rapid MR imaging. Magn Reson Medicine: Official J Int Soc Magn Reson Med. 2007;58:1182–95.
27. Tsai C-M. Nishimura. Reduced aliasing artifacts using variable-density k-Space sampling trajectories. Magn Reson Med. 2000;43:452–8.
28. Dwork N, Baron CA, Johnson EMI, O'Connor D, Pauly JM, Larson PEZ. Fast variable density Poisson-disc sample generation with directional variation for compressed sensing in MRI. Magn Reson Imaging. 2021;77:186–93. https://doi.org/10.1016/j.mri.2020.11.012. Epub 2020 Nov 21. PMID: 33232767; PMCID: PMC7878411.
29. Greiser A, von Kienlin M. Efficient k-space sampling by density-weighted phase-encoding. Magn Reson Med. 2003;50:1266–75.
30. Otazo R, Kim D, Axel L, Sodickson DK. Combination of compressed sensing and parallel imaging for highly accelerated first-pass cardiac perfusion MRI. Magn Reson Med. 2010;64:767–76.
31. Klaas P, Pruessmann M, Weiger P, Bornert, Boesiger P. Advances in sensitivity encoding with arbitrary k-space trajectories. Magn Reson Med. 2001;46:638–51.
32. Stone SS, Haldar JP, Tsao SC, Hwu WM, Sutton BP, Liang ZP. Accelerating Advanced MRI Reconstructions on GPUs. J Parallel Distrib Comput. 2008;68(10):1307–18. https://doi.org/10.1016/j.jpdc.2008.05.013. PMID: 21796230; PMCID: PMC3142623.
33. Pedersen H, Kozerke S, Ringgaard S, Nehrke K. Kim. k-t PCA: temporally constrained k-t BLAST reconstruction using principal component analysis. Magn Reson Med. 2009;62:706–16.
34. Miller S, Simonetti OP, Carr J, Kramer U, Finn JP. MR Imaging of the heart with cine true fast imaging with steady-state precession: influence of spatial and temporal resolutions on left ventricular functional parameters. Radiology. 2002;223(1):263-9. doi: https://doi.org/10.1148/radiol.2231010235. PMID: 11930076.
35. Sievers B, Addo M, Kirchberg S et al. Impact of the ECG gating method on ventricular volumes and ejection fractions assessed by cardiovascular magnetic resonance imaging. J Cardiovasc Magn Reson. 2005;7(2):441-6. doi: 10.1081/jcmr-200053515. Erratum in: J Cardiovasc Magn Reson. 2005;7(5):871-2. PMID: 15881527.
36. Han Y, Osborn EA, Maron MS, Manning WJ, Yeon SB. Impact of papillary and trabecular muscles on quantitative analyses of cardiac function in hypertrophic cardiomyopathy. J Magn Reson Imaging. 2009;30(5):1197 – 202. doi: https://doi.org/10.1002/jmri.21958. PMID: 19856455.
37. Fathi A, Weir-McCall JR, Struthers AD, Lipworth BJ, Houston G. Effects of contrast administration on cardiac MRI volumetric, flow and pulse wave velocity quantification using manual and software-based analysis. Br J Radiol. 2018;91(1084):20170717. https://doi.org/10.1259/bjr.20170717. Epub 2018 Jan 19. PMID: 29271236; PMCID: PMC5965987.
38. Malayeri AA, Johnson WC, Macedo R, Bathon J, Lima JA, Bluemke DA. Cardiac cine MRI: quantification of the relationship between fast gradient echo and steady-state free precession for determination of myocardial mass and volumes. J Magn Reson Imaging. 2008;28(1):60–6. https://doi.org/10.1002/jmri.21405. PMID: 18581356; PMCID: PMC2671062.
39. Zou Q, Xu HY, Fu C, et al. Utility of single-shot compressed sensing cardiac magnetic resonance cine imaging for assessment of biventricular function in free-breathing and arrhythmic pediatric patients. Int J Cardiol. 2021;338:258–64. https://doi.org/10.1016/j.ijcard.2021.06.043. Epub 2021 Jun 26. PMID: 34181995.
40. Curione D, Ciliberti P, Monti CB, et al. Compressed sensing Cardiac Cine Imaging compared with standard balanced steady-state free precession cine imaging in a Pediatric Population. Radiol Cardiothorac Imaging. 2022;4(2):e210109. https://doi.org/10.1148/ryct.210109. PMID: 35506130; PMCID: PMC9059096.
41. Chen X, Pan J, Hu Y, Hu H, Pan Y. Feasibility of one breath-hold cardiovascular magnetic resonance compressed sensing cine for left ventricular strain analysis. Front Cardiovasc Med. 2022;9:903203. https://doi.org/10.3389/fcvm.2022.903203. PMID: 36035944; PMCID: PMC9411808.

Publisher's Note